

## CRACK FRONT PENETRATION IN TRANSGRANULAR CLEAVAGE CRACKING IN AN IRON–SILICON ALLOY

W. Lu, J. Chen, and Y. Qiao

UDC 539

**Abstract:** Based on the analysis of the crack trapping effect of cleavage ridges and penetration of crack front segments in an iron–silicon alloy, the distance between break-through points along a high-angle grain boundary is investigated. If the break-through points are close to each other, the crack trapping effect is dominant; otherwise, the grain boundary separation in break-through windows governs the front transmission process. The relationship between the overall grain boundary fracture resistance and the break-through-point distance is quite complex. The minimum grain boundary resistance is achieved when the break-through points are about 2–3  $\mu\text{m}$  apart, which is also influenced by the grain boundary shear strength, the crystallographic toughness and orientation, as well as the crack front profile.

*Keywords:* grain boundary, fracture resistance, cleavage.

**DOI:** 10.1134/S0021894412030194

## INTRODUCTION

In a recent experimental study on cleavage cracking in polycrystalline materials [1–4], it was observed that a cleavage crack overcame a high-angle grain boundary by crack front branching. When the crack-tip stress intensity was relatively low, the front would stably penetrate through the boundary. The penetrating front segments bowed into the second grain, and the penetration depth and the width of break-through windows increased with the external loading. The break-through points (BTPs) were distributed along the boundary quite regularly, while occasionally the BTP distance could be relatively large. Eventually, when the crack growth driving force, i.e., the energy release rate ( $G$ ) reached the critical value, the cleavage front transmission process was completed and the crack would propagate forward unstably.

Understanding grain boundary toughness is critical to improving fracture resistances of brittle polycrystalline materials where transgranular cleavage is the primary failure mode. For instance, in the classical fracture mechanics, it is often assumed that failure of a brittle material is triggered by unstable growth of one or a few grain-sized microcracks [5]. The microcracks are grain-sized because they are arrested by grain boundaries, clearly indicating that grain boundaries are the main barriers that they must overcome. Thus, the critical condition for cracks to grow across grain boundaries, i.e., the grain boundary fracture resistance, dominates the overall failure criterion.

One intrinsic factor that governs the interaction between the crack front and the grain boundary is the distance between adjacent BTPs ( $w$ ). According to the fractography study [3], for an iron–silicon alloy the most probable value is  $w = 2\text{--}3 \mu\text{m}$ . Break-through points closer than  $0.2 \mu\text{m}$  were not observed, while  $w$  could be much

---

Department of Structural Engineering, University of California, San-Diego, La Jolla, CA 92093-0085; yqiao@ucsd.edu. Translated from *Prikladnaya Mekhanika i Tekhnicheskaya Fizika*, Vol. 53, No. 3, pp. 176–183, May–June, 2012. Original article submitted May 19, 2011.

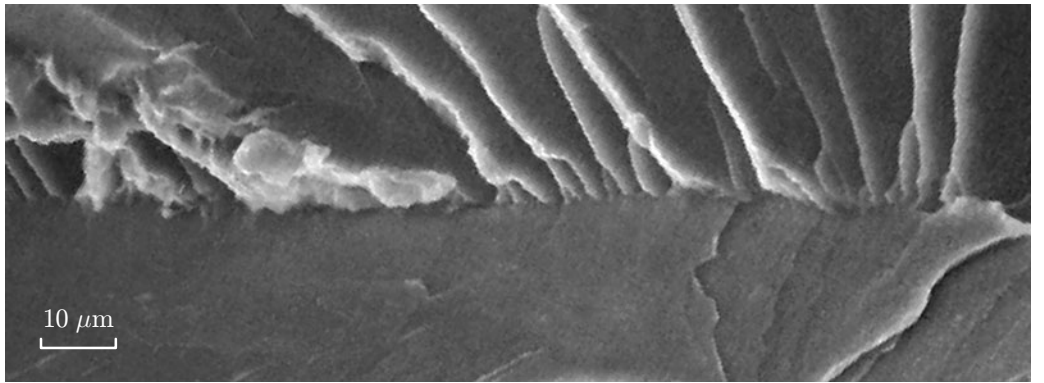


**Fig. 1.** SEM microscopy of cleavage cracking across a high-angle grain boundary in an iron–silicon alloy (the crack propagates from the bottom to the top, as is indicated by the arrow).

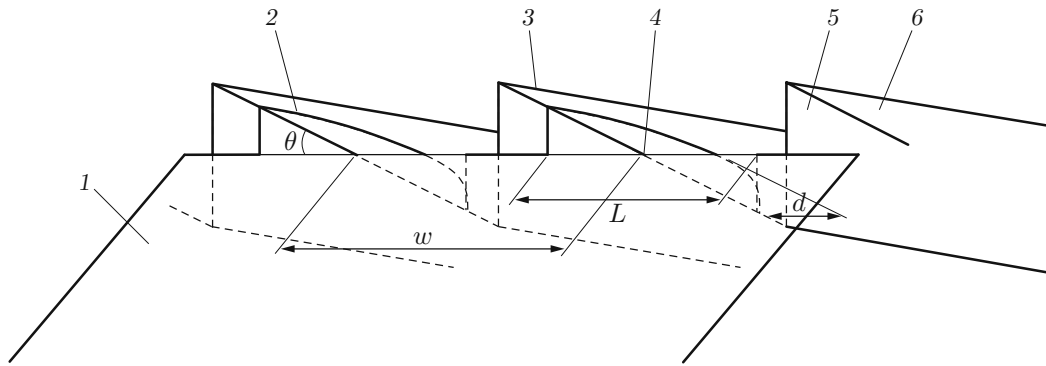


**Fig. 2.** Schematic diagram of a cleavage front penetrating across a high-angle grain boundary: (1) cleavage plane in the first grain; (2) cleavage front segment penetrating through the boundary; (3) cleavage ridge; (4) break-through point; (5) grain boundary; (6) cleavage plane in the second grain.

larger, in the range of 10–80  $\mu\text{m}$ , in some sections of the boundary, as is shown in Fig. 1. In an “ideal” case where  $w$  was infinitesimal, the BTPs are immediately next to each other, and the area of the grain boundary involved in the front transmission is negligible, so the fracture work is required for BTP separation. While this explains that large values of  $w$  were only seldom observed, it cannot answer the question why  $w$  was not smaller than the experimental result. Note that the characteristic length scale of the grain boundary structure is much lower than 2–3  $\mu\text{m}$  [6]. Furthermore, it was noticed that there were no abrupt changes in directions of river markings associated with variations in the BTP distance; that is, the chronology of crack front advance across the grain boundary, which is related to the local fracture resistance, is insensitive to the BTP distance in the range of the measured values.

In this article, we show that a critical BTP distance,  $w_{\text{cr}}$ , can be obtained by taking into consideration both the crack trapping effect of cleavage ridges and the competition between variations in the crack growth driving force and local fracture resistance. Other factors, such as the grain boundary shear strength, the crystallographic orientation and fracture resistance, as well as the crack front profile, come in by affecting the critical BTP distance.

## 1. CRACK FRONT PENETRATION ACROSS A HIGH-ANGLE GRAIN BOUNDARY

As it was discussed above, before a high-angle grain boundary is fully overcome, the cleavage front can penetrate through it at the BTP points (Fig. 2). Because the crystallographic orientations of the two grains across the boundary are different, the crack front is broken down into a number of segments, each around a BTP. The front segments advance on the primary cleavage plane in the grain ahead of the boundary. Eventually when the

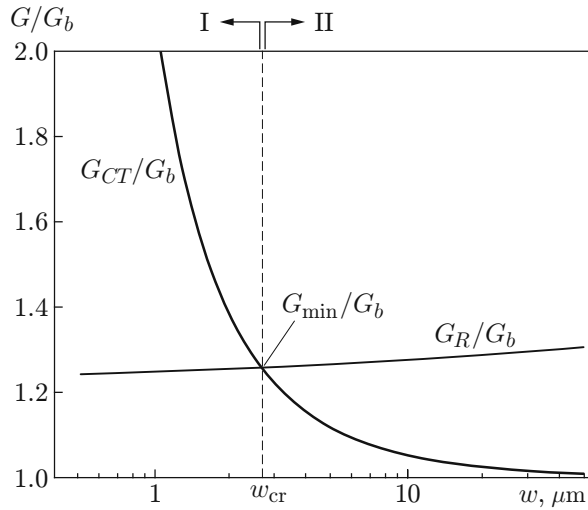


**Fig. 3.** Competition between the two grain boundary separation mechanisms: the crack-trapping dominated and  $R$ -curve dominated domains are indicated by I and II, respectively.

two crack flanks are separated apart, secondary fracture must take place along the direction normal to the primary fracture surface, leading to the formation of river markings (cleavage ridges). The river markings show the profile of the advancing cleavage front. As the front segment bows into the second grain, the grain boundary around the BTP is also separated apart, forming a break-through window. According to the experimental measurements [7], the width of the break-through window is described by the power-law relation  $L/w = \alpha(d/w)^\beta$ , where  $L$  is the break-through window width,  $d$  is the break-through depth,  $\alpha \approx 3.5$ , and  $\beta \approx 0.6$ . If the front penetration is continuous, the areas of the grain boundary separated apart in break-through windows and the cracked zones in crystallographic planes increase with increasing crack propagation rates; therefore; the effective fracture resistance ( $R$ ) rises; that is, the crack growth driving force ( $G$ ) must increase to drive the front segments moving forward. The critical condition is  $G = R$ . Note that  $G$  also increases with  $d$  at a constant external loading. However, initially, when the front penetration depth is relatively small ( $dG/dd < dR/dd$ ), the crack front advances by infinitesimal steps ( $G < R$ ). Thus, the crack stops until the external loading is further increased. Under this condition, the crack front penetration is stable. As  $d$  increases, when  $dG/dd \geq dR/dd$ , the front advance becomes unstable, since  $G > R$  as the crack further grows. In this well-established framework of the  $R$ -curve analysis (see, e.g., [8]), the effective grain boundary fracture resistance should be taken as the value of  $R$  at which the conditions  $G = R$  and  $dG/dd = dR/dd$  are satisfied simultaneously, which can be calculated as [7]

$$G_R/G_b = C_1(1 + 0.12k_0C_2)^2,$$

where  $C_1 = \cos\theta(\sin\theta + \cos\theta)$  and  $C_2 = [\sin^2\theta \cos^2\theta \cos\psi / (\sin\theta + \cos\theta)]^{1.05}$  are two parameters dependent on crystallographic misorientations across the boundary,  $\theta$  and  $\psi$  are the twist and tilt misorientation angles, respectively,  $G_b = G_{ICSC} / (\cos\theta \cos\psi)$  is the effective fracture resistance of the grain ahead of the boundary,  $G_{ICSC}$  is the crystallographic fracture resistance,  $k_0 = [(a_0/w)^m (\alpha^3/8)(k/\mu)(kw/G_{ICSC})]^{1.05}$ ,  $a_0$  is the initial crack length,  $k$  is the effective shear strength of the grain boundary,  $m = 3\beta - 1$ , and  $\mu$  is the effective shear modulus. For the iron–silicon alloy studied by Qiao and Argon [3],  $k = 144$  MPa,  $k/\mu \approx 0.1\%$ ,  $a_0 = 60$  mm, and  $G_{ICSC} = 850$  J/m. It can be seen that  $G_R$  is an increasing function of  $w$  (Fig. 3). The values of  $\theta$  and  $\psi$  are set to the middle points of their possible ranges, i.e.,  $\theta = 22.5^\circ$  and  $\psi = 22.5^\circ$ .

While the grain boundary in break-through windows can be separated apart spontaneously when the front penetrates across the boundary, the part around the secondary fracture surfaces, i.e., the river markings, must be broken apart by shearing. At the intersection of two cleavage terraces, the primary cleavage plane is discontinuous, and the front propagation within the grain boundary plane, which may be regarded as a mode-III fracture process, is interrupted; that is, cleavage ridges at the boundary can act as bridging reinforcements locally pinning together the two fracture flanks, offering additional fracture resistance. As a crack front segment penetrates between two cleavage ridges, the local stress intensity at the protruding part is smaller than the nominal value [9]. The excess

crack growth driving force is carried by cleavage ridges that are left behind the verge of the propagating front. To keep the crack front advancing, the local crack growth driving force must be equal to the local fracture resistance and the value of  $G_b$  (material constant) must be larger than the nominal crack-tip stress intensity. Otherwise, the front would stop. Hence, the effective fracture resistance of a crystalline material is higher than that of a homogenous material. Eventually, as the two front segments at both sides of a cleavage ridge merge together, somewhat similar to a cleavage crack bypassing a regular array of tough reinforcements in a composite material [10, 11], the grain boundary is broken through. Based on an energy analysis by Kong and Qiao [12], the critical energy release rate required to overcome the crack trapping effect of cleavage ridges can be calculated as

$$\frac{G_{CT}}{G_b} = \left(1 - \frac{D}{w}\right) + \left[1.7 + 2.4 \frac{D}{w} + 0.1 \left(\frac{D}{w}\right)^2\right]^2 \frac{D}{w},$$

where  $D$  is the width of the cleavage ridge, which, according to a fractography study, was about  $0.25 \mu\text{m}$  for the iron–silicon alloy. The relationship between the grain boundary fracture resistance caused by crack trapping by cleavage ridges,  $G_{CT}$ , and  $w$  is shown in Fig. 3. It can be seen clearly that  $G_{CT}$  decreases as  $w$  increases, which should be attributed to the fact that a large number of cleavage ridges is formed along the boundary if the BTPs are close to each other.

## 2. BREAK-THROUGH-POINT DISTANCE AND GRAIN BOUNDARY FRACTURE RESISTANCE

As it was discussed above, there are two mechanisms of grain boundary separation associated with cleavage cracking: spontaneous grain boundary separation in break-through windows and shearing of the grain boundary on cleavage ridges. The barrier effect of the boundary is fully overcome only when both boundary separation processes are completed. Note that they lead to different dependences of  $w$  on grain boundary resistance. When  $w$  is relatively small,  $G_{CT}$  decreases rapidly as  $w$  increases, and its value converges to  $G_b$  as  $w$  becomes relatively large. On the other hand,  $G_R$  increases with  $w$ ; however, the increase rate is quite small compared with the decrease rate of  $G_{CT}$  in a small range of  $w$ . At the critical value of  $w$  ( $w_{cr} = 2.6 \mu\text{m}$ ), the equality  $G_{CT} = G_R$  holds. At  $w < w_{cr}$ , the inequality  $G_{CT} > G_R$  is valid. Under this condition, when the nominal energy release rate,  $G$ , reaches  $G_R$ , the grain boundary in break-through windows fails, while  $G$  must be further raised to  $G_{CT}$  to complete the boundary separation at cleavage ridges. Thus, the effective grain boundary fracture resistance is  $G_{GB} = G_{CT}$ , i.e., the grain boundary failure is dominated by the crack trapping effect. When  $w > w_{cr}$ , we have  $G_{CT} < G_R$ ; that is, if  $G = G_R$ , not only the crack front in break-through windows becomes unstable, but also cleavage ridges can be overcome. Therefore, the effective grain boundary fracture resistance should be taken as  $G_R$ , i.e., the boundary failure is dominated by the critical condition of unstable advance of penetrating crack front segments.

It can be seen that the grain boundary fracture resistance is minimum at  $w = w_{cr}$ , indicating that  $w_{cr}$  is the most energetically favorable BTP distance for the cleavage front to transmit across the grain boundary. The minimum value,  $G_{min}$ , is about  $1.3G_b$ , close to the experimental data of grain boundary resistance; the value of  $w_{cr}$  fits well with the testing data of the modes of the distribution curves of the BTP distance [3].

As  $w$  decreases from  $w_{cr}$ ,  $G_{GB} = G_{CT}$  increases significantly. At  $w = 1 \mu\text{m}$ , the value of  $G_{GB}$  is nearly doubled as compared with  $G_{min}$ . Hence, it is highly unlikely that BTPs can be closer to each other than  $w_{cr}$ . Even if the initial BTP distance is smaller than  $w_{cr}$ , due to the difficulty in cleavage ridge shearing, the BTPs of relatively high local fracture resistances would be deactivated, until the effective BTP distance is increased to  $w_{cr}$ , at which cleavage ridge failure and the break-through window separation take place at the same energy release rate.

As  $w$  increases from  $w_{cr}$ , the effective grain boundary fracture resistance,  $G_{GB} = G_b$ , increases; therefore, if the BTPs are far from each other, a higher energy release rate is required. As the external loading increases, the cleavage front can penetrate across the boundary through a greater number of BTPs, resulting in a smaller value of  $w$ . As  $G_{GB}$  decreases with  $w$ , the energy barrier for the crack to bypass the grain boundary is lower and lower. Eventually, at  $G = G_{GB}$ , the cleavage front transmission process, both in break-through windows and at cleavage ridges, is completed. Note that the  $G_R$  variation rate is quite small compared with that of  $G_{CT}$  in the range  $w < w_{cr}$ . Therefore, larger values of  $w$  could be observed occasionally in experiments (see Fig. 1), since the associated increase in fracture resistance can be relatively easily overcome by a local increase in the crack growth driving force.

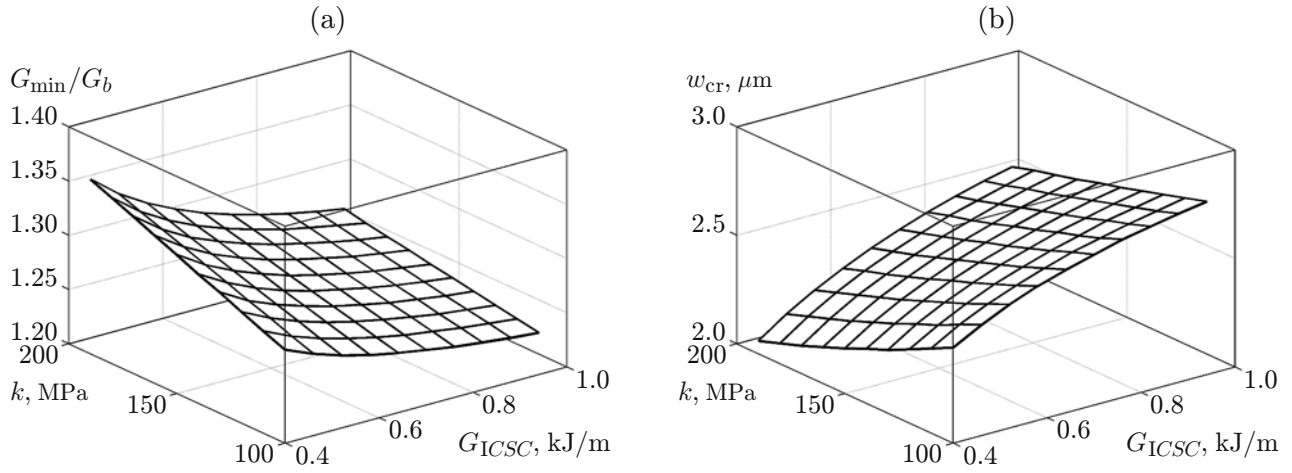


**Fig. 4.** Minimum grain boundary fracture resistance (a) and break-through point distance (b) as functions of  $k$  and  $G_{ICSC}$ .

In addition to the BTP distance, there are a number of other important factors, including the effective shear strength of the grain boundary,  $k$ , and the effective work of separation of the crystallographic plane,  $G_{ICSC}$ , which come in by affecting  $G_R$ . Their effects on  $G_{min}$  and  $w_{cr}$  are shown in Figs. 4a and 4b, respectively. As  $G_{ICSC}$  increases, a greater fracture work needs to be done to separate apart crystallographic planes; therefore, the importance of the grain boundary is lowered, leading to decreasing curves of grain boundary fracture resistance as a function of  $k$  and  $G_{ICSC}$ . More specifically, when the crystallographic toughness rises, compared with the front advance in the primary cleavage plane, the expansion of break-through window along the grain boundary is less difficult; therefore, the value of the parameter  $k_0$  decreases, and so does  $G_R$ . Thus,  $G_{min}$  decreases, while  $w_{cr}$  increases, i.e., the BTPs tend to be farther apart from each other. Note that the influence of  $G_{ICSC}$  on  $G_{GB}$  is pronounced only at  $w > w_{cr}$ . If  $w$  is relatively small, the  $G_{CT}$  curve is not affected.

If the grain boundary shear strength increases, since the front transmission in break-through windows becomes more difficult,  $G_{min}$  increases. Accordingly,  $w_{cr}$  decreases, since the area of the separated grain boundary is smaller at the same nominal stress intensity, and BTPs must be closer to each other; otherwise, the grain boundary could not be fully separated apart. Similar to the crystallographic fracture resistance, the factor of  $k$  is active only at  $w > w_{cr}$ . When the BTP distance is relatively small, the crack trapping effect is dominant and the front behavior in break-through windows is no longer important. Note that the effects of  $k$  on  $G_{min}$  and  $w_{cr}$  are more significant than that of  $G_{ICSC}$ , which can be attributed to the fact that  $k$  directly affects the work of separation of the grain boundary while  $G_{ICSC}$  only changes the distribution of the work on separation of fracture surfaces.

In the above-performed discussion, it is assumed that the profile of the crack front segment that penetrates across the grain boundary is known. According to the experimental measurement [7], the geometry factor,  $\beta$ , is larger than 0.5, close to 0.6, i.e., the penetrating front segment is “narrower” and “sharper” than a semi-circle. As the value of  $\beta$  increases, the width of the break-through window is smaller at the same penetration depth, and the verge of the penetrating crack front must protrude deeper into the grain ahead of the boundary to separate apart the entire grain boundary. The BTPs tend to be closer to each other, resulting in a descending  $w_{cr}(\beta)$  curve (dashed curve in Fig. 5). Thus, to break through the same grain boundary, a larger nominal crack growth driving force must be applied, causing an increasing  $G_{min}(\beta)$  curve (solid curve) in Fig. 5 with decreasing distance. However, as  $\beta$  changes, the variations in  $w_{cr}$  and  $G_{min}$  are small. For instance, as  $\beta$  increases from 0.5 to 0.6,  $G_{min}/G_b$  increases by only less than 5%, indicating that the front profile effect is secondary compared with the influence of  $w$ ,  $k$ , and  $G_{ICSC}$ .

Other important factors include the crystallographic misorientation angles across the boundary, which come in by affecting the fracture resistance of the second grain ( $G_b$ ) as well as the orientation parameters  $C_1$  and  $C_2$ . An increase in either  $\theta$  or  $\psi$  would cause an increase in grain boundary fracture resistance, and the effect of the twist angle is more pronounced [2, 3, 7, 13].

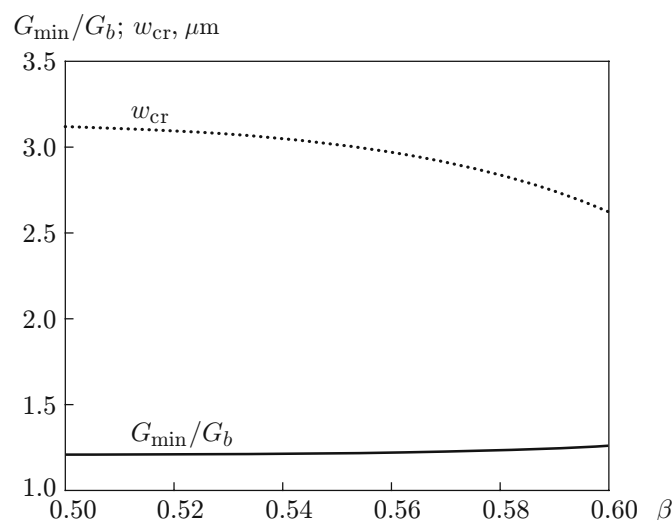


**Fig. 5.** Break-through point distance and minimum grain boundary fracture resistance as functions of the cleavage front geometry factor.

## CONCLUSIONS

In the current study, the separation of a high-angle grain boundary with a cleavage crack penetrating across it is discussed. The grain boundary area in break-through windows can be separated apart spontaneously as the penetrating crack front segments advance in the grain ahead of the boundary, and the grain boundary areas at cleavage ridges must be broken apart via shearing. The former mechanism is dominated by the competition between the increase in local fracture resistance and the increase in the crack growth driving force; the latter mechanism is dominated by the crack trapping effect. Both of the two barrier effects must be overcome so that the cleavage front can bypass the grain boundary, which is highly dependent on the distance between break-through points. When the break-through-point distance is relatively small, the grain boundary failure is governed by the crack trapping effect, and the effective grain boundary fracture resistance increases rapidly as the BTP distance decreases; when the BTP distance is relatively large, the grain boundary fracture resistance, which increases slightly with the BTP distance, is determined by the break-through window behavior. At the critical BTP distance, the resistance offered by the grain boundary to cleavage cracking is minimized. Other important factors include the grain boundary shear strength, crystallographic fracture resistance, and crystallographic orientations, compared with which the influence of the crack front profile is secondary.

This work was supported by the Department of Energy (Grant No. DE-FG02-05ER46195).

## REFERENCES

1. A. S. Argon and Y. Qiao, "Resistance of Cleavage Cracking of High-Angle Bicrystal Grain Boundaries in Fe-Si Alloy," *Philos. Mag. A*, No. 82, 3333–3348 (2002).
2. Y. Qiao and A. S. Argon, "Cleavage Crack-Growth-Resistance of Grain Boundaries in Polycrystalline Fe-2 wt% Si Alloy: Experiments and Modeling," *Mech. Mater.*, No. 35, 129–154 (2003).
3. Y. Qiao and A. S. Argon, "Cleavage Cracking Resistance of High Angle Grain Boundaries in Fe-3 wt% Si Alloy," *Mech. Mater.*, No. 35, 313–331 (2003).
4. Y. Qiao and A. S. Argon, "Brittle-to-Ductile Fracture Transition in Fe-3 wt% Si Single Crystals by Thermal Crack Arrest," *Mech. Mater.*, No. 35, 903–912 (2003).
5. F. A. McClintock and A. S. Argon, *Mechanical Behaviors of Materials* (CBLs, Marietta, 1993).
6. P. E. J. Flewitt and R. K. Wild, *Grain Boundaries: Their Microstructures and Chemistry* (John Wiley and Sons, New York, 2001).

7. Y. Qiao, "Modeling of Resistance Curve of High-Angle Grain Boundary in Fe-3 wt% Si Alloy," *Mater. Sci. Eng. A*, No. 361, 350-357 (2003).
8. T. L. Anderson, *Fracture Mechanics: Fundamentals and Applications* (CRC Press, Boca Raton, 2004).
9. J. R. Rice, "First-Order Variation in Elastic Fields due to Variation in Location of a Planar Crack Front," *Trans. ASME, J. Appl. Mech.*, No. 52, 571-579 (1985).
10. A. F. Bower and M. A. Ortiz, "3-Dimensional Analysis of Crack Trapping and Bridging by Tough Particles," *J. Mech. Phys. Solids* **39** (6), 815-858 (1991).
11. T. M. Mower and A. S. Argon, "Experimental Investigations of Crack Trapping in Brittle Heterogeneous Solids," *Mech. Mater.*, No. 19, 343-364 (1995).
12. X. Kong and Y. Qiao, "Crack Trapping Effect of Persistent Grain Boundary Islands," *Fatigue Fract. Eng. Mater. Struct.*, No. 28, 753-758 (2005).
13. Y. Qiao, J. K. Deliwala, S. S. Chakravarthula, and X. Kong, "High-Temperature Tensile Properties of a Polymer Intercalated/Exfoliated Cement," *Mater. Lett.*, No. 59, 3616-3619 (2005).